Fuel 165 (2016) 205–214

Contents lists available at ScienceDirect

Fuel

journal homepage: www.elsevier.com/locate/fuel

Prediction of high-temperature rapid combustion behaviour of woody biomass particles

Jun Li [a,*,1], Manosh C. Paul [a,*], Paul L. Younger [a], Ian Watson [a], Mamdud Hossain [b], Stephen Welch [c]

[a] Systems, Power & Energy Research Division, School of Engineering, University of Glasgow, Glasgow G12 8QQ, UK
[b] School of Engineering, Robert Gordon University, Aberdeen AB10 7QB, UK
[c] BRE Centre for Fire Safety Engineering, School of Engineering, University of Edinburgh, Edinburgh EH9 3JL, UK

ARTICLE INFO

Article history:
Received 14 February 2015
Received in revised form 15 October 2015
Accepted 15 October 2015
Available online 23 October 2015

Keywords:
Biomass
Combustion
High temperature
Single particle model

ABSTRACT

Biomass energy is becoming a promising option to reduce CO_2 emissions, due to its renewability and carbon neutrality. Normally, biomass has high moisture and volatile contents, and thus its combustion behaviour is significantly different from that of coal, resulting in difficulties for large percentage biomass co-firing in coal-fired boilers. The biomass combustion behaviour at high temperatures and high heating rates is evaluated based on an updated single particle combustion model, considering the particle size changes and temperature gradients inside particle. And also the apparent kinetics determined by high temperature and high heating rate tests is employed to predict accurate biomass devolatilization and combustion performances. The time-scales of heating up, drying, devolatilization, and char oxidation at varying temperatures, oxygen concentrations, and particle sizes are studied. In addition, the uncertainties of swelling coefficient and heat fractions of volatile combustion absorbed by solid on the devolatilization time and total combustion time are discussed. And the characterised devolatilization time and total combustion time are finally employed to predict the biomass combustion behaviour. At the last, a biomass combustion/co-firing approach is recommended to achieve a better combustion performance towards large biomass substitution ratios in existing coal-fired boilers.

1. Introduction

Biomass is a potential fuel that can deliver a significant reduction in net carbon emissions when compared with fossil fuels, and additional environmental and social benefits could also be expected [1]. However, the combustion properties of biomass are significantly different to those of coals, due to its high volatile contents and low energy densities. The challenges of the large percentage biomass co-firing (over 20% on energy basis) in existing pulverized coal boilers are keeping the same steam parameters and having a high boiler efficiency and a stable operation. Typically, when co-firing biomass e.g. in an existing coal-fired boiler, drag forces acting upon the biomass particles are more important than that acting on coal particles, which can cause unexpected flame patterns compared to coal flames. Therefore, elucidation of the combustion mechanism is key to understanding biomass combustion per se, as well as in co-firing behaviours.

The single particle model (SPM) has widely been employed to study coal combustion, rapid pyrolysis and devolatilization, char gasification and combustion, ignition delay, and combustion timescale [2–14]. Recently, Haseli et al. [10] studied the combustion of a woody biomass particle using a detailed one-dimensional model accounting for particle heating-up, devolatilization, char oxidation, and gaseous phase reactions within and in the vicinity of particle. Lu et al. [11,12] employed a one-dimensional particle model to investigate the effects of particle size and particle shape (sphere, cylinder, and flat plate) on devolatilization and combustion performance of biomass. Saastamoinen et al. [13] investigated biomass burnout properties using a simplified single particle approach and compared results with those of coal and concluded that the particle size of biomass can be much larger than that of coal to reach a complete burnout due to its lower density and greater reactivity. Yang et al. [14] studied combustion characteristics of a single biomass particle, considering a wide range of size from 10 μm to 20 mm using mathematical modelling approaches and compared their results with experimental data.

When the biomass particles enter a pulverized fuel flame, they are rapidly heated to a final temperature in the range of 1400–1600 °C at a rate of about 10^4 °C/s [15]. In fact, experimental

* Corresponding authors. Tel.: +44 (0)141 330 8466.
E-mail addresses: Jun.Li@glasgow.ac.uk (J. Li), Manosh.Paul@glasgow.ac.uk (M.C. Paul).
[1] Present address: Department of Chemical and Process Engineering, University of Strathclyde, Glasgow G1 1XJ, UK.

http://dx.doi.org/10.1016/j.fuel.2015.10.061
0016-2361/

Nomenclature

Symbols

A	pre-exponential factor in Arrhenius expression (1/s)
C	carbon content (%, dry ash free basis)
D	diffusion rate coefficient (m^2/s)
d_p	particle diameter (m)
E	activation energy (J/kmol)
f	faction of heat absorbed by solid residuals
k	kinetic constant (kg/m^2 Pa s)
$\dot{k}$	thermal conductivity (W/m K)
m	mass (kg)
MC	moisture content (%)
n	reaction order (–)
P	pressure (Pa)
$\widetilde{Q}$	reaction heat absorbed by solid remains (J)
r	particle radius (m)
R	gas universal constant, 8.3143 J/(mol K)
S	char specific surface (m^2/kg)
T	temperature (K)
X	mass conversion (–)
α	particle size evolution exponent (–)

Subscripts

DB	dry biomass
dry	drying
devo	devolatilization
exp	experimental
g	gas phase
M	moisture
mod	modelled
ox	char oxidation
p	particle
s	solid remains
vola	volatile
w	furnace wall
0	initial value

measurement of mass loss during biomass thermal conversions, especially at high temperature and high heating rate, is always challenging and seldom reported. To achieve a better co-firing flame profile and thus an enlarged biomass co-firing ratio, the devolatilization and char oxidation behaviour of biomass are expected to be similar or comparable to that of coal. The devolatilization time and the char oxidation time are two essential parameters, the devolatilization time often reflects the lift-off distance of a flame, and the char oxidation time influences the flame profile. By combination of these two timescale parameters with transport phenomenon, it is possible to analyse or compare the flame profiles of various fuels inside the furnace. However, existing biomass combustion models might lead to inaccurate predictions on devolatilization time and char oxidation time, for examples, the particle size changes during biomass thermal conversions haven't been considered in most models, although some modes considered only particle size changes at char oxidation stage either by shrinking (constant density) core approach [12] or empirical correlations [10], but neglecting the particle size changes at devolatilization process; uniform temperature was often assumed in biomass combustion simulations, which could cause significantly incorrect predictions of thermal conversation process for larger particles; in addition, most available kinetics data for biomass devolatilization and char oxidation were commonly determined by TGA tests, during which the low heating rates limit the rates of mass and heat transfers, the kinetics determined at near real conditions are required to accurately address biomass combustion [15].

In this work, the biomass combustion behaviour is evaluated based on an updated single particle model, considering the particle size changes and temperature gradients inside particle. And also the apparent kinetics determined by high temperature and high heating rate tests is employed, aiming for accurate predictions of biomass combustion behaviour with the capability of representing more faithfully combustion behaviour at true boiler furnace conditions. The timescales of heating up, drying, devolatilization, and char oxidation at varying temperatures, oxygen concentrations, and particle sizes are studied. In addition, the uncertainties of swelling coefficient and heat fractions of volatile combustion absorbed by solid on the devolatilization time and total combustion time are discussed. Finally, the characterised devolatilization time and total combustion time are employed to analyse the biomass combustion behaviour.

2. Materials and methods

2.1. Fuel properties

In this work, the studied biomass has been investigated experimentally its devolatilization and char oxidation properties at high temperatures and high heating rates [15,16]. The proximate and ultimate analysis of the studied biomass and coal (for comparison) are presented in Table 1.

2.2. Modelling approach

The objective of this study concerns exposing a biomass particle in a high temperature furnace; the oxidising agent at furnace temperature with specified oxygen concentration comes from one side of the furnace, and the flue gas flows out from the other side after combustion with biomass particle. The whole combustion process includes (Fig. 1): the particle heating-up to the furnace temperature; drying; devolatilization; volatile combustion, and char oxidation.

Once exposed in the high temperature furnace, the biomass particle is heated up by the surrounding furnace wall and oxidising agent via radiation and convection, resulting in a rise in the surface temperature of the biomass particle. The released heat is then transferred from the particle surface to its centre in terms of heat conduction, and the conductivity of biomass is a function of temperature and solid residues such as char and ash. The temperature gradient inside particle is considered, the drying and devolatilization start when local temperature inside particle reaches respective reactions temperature. The drying and devolatilization rates increase when particle temperature increasing, and the drying and devolatilization may occur simultaneously until the biomass particle is completely dried.

The released amount of volatile matter depends on the fuel type and devolatilization conditions e.g. final temperature and heating rates, the volatiles at high temperatures mainly consists of gaseous hydrocarbons. In this study, volatile is treated as a non-conventional material, like biomass, which consists of C, H, O, and N. The updated model can automatically calculate contents of elements and heating value of volatile based on the proximate and ultimate data, and therefore the model is flexible for studies of various types of biomass. Although the volatiles comprise a range of species, it is reasonable to represent the volatile matter

Table 1
Fuel properties.

	Proximate analysis (wt%)				Ultimate analysis (wt%)				LHV^{db} (MJ/kg)
	Moisture^{ar}	Volatile^{db}	FC^{db}	Ash^{db}	C^{db}	H^{db}	O^{db}	N^{db}	
Biomass	5.60	61.87	30.82	7.31	55.43	4.90	31.83	0.50	20.5
Coal	1.43	27.85	47.09	25.06	60.26	3.97	8.33	1.27	24.0

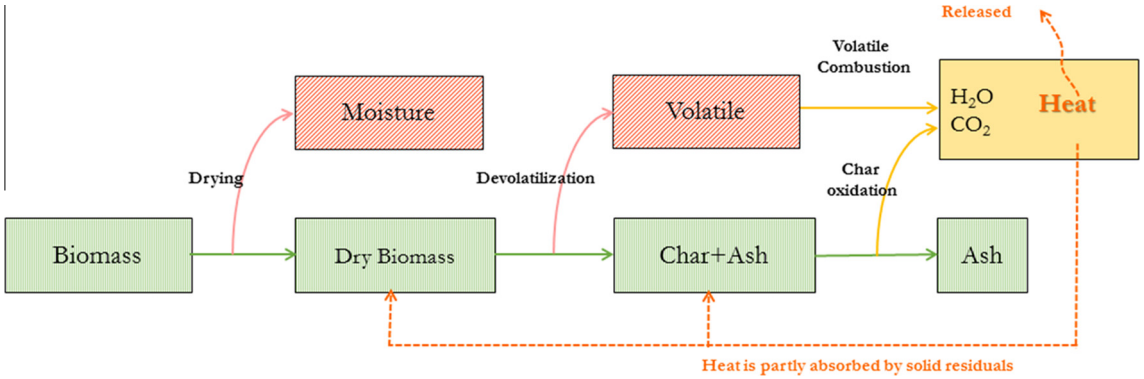

Fig. 1. Reaction pathway of biomass particle combustion.

as a single virtual material [17], because the releasing kinetics of individual gaseous species during devolatilization are still not clear, due to the complexities of chemical reactions regarding to various intermediates and final gaseous products; moreover, typically in the case of combustion, the complicated formation mechanism of volatile species is not necessarily needed because combustible gases are combusted immediately under sufficient oxygen and high temperature conditions, aiming to reduce computational cost.

In this study, the agent flow sweeps the particle with a certain velocity, and thus the volatile combustion occurs close to the particle but not surrounded on the surface area, and therefore heat fraction of volatile combustion absorbed by solid remains as an uncertainty. To have a clear understanding in the impacts of heat from volatile combustion on the biomass combustion process, uncertainty analysis of heat fraction of volatile combustion absorbed by solid are performed. After the devolatilization, the char and ash remain as solid residues. The principal assumptions made in this model are as follows: (1) all range size (0.1–10 mm) particles are assumed as spherical with aim of studies of the impacts of particles size on biomass combustion behaviour; (2) due to the apparent kinetics applied to the model, the changes of particle porosity are thus neglected; (3) the drying process is independent of the combustion process.

2.3. Mass and energy conservations

The equations presented below describe the evolution of solid components considering dry biomass (DB), char and ash. The equations describing the evolution of the solid components (dry biomass, char, and ash) are:

$$\frac{\partial \rho_{DB}}{\partial t} = -k_{devo}\rho_{DB} \tag{1}$$

$$\frac{\partial \rho_{Char}}{\partial t} = (1 - v_{Vola})k_{devo}\rho_{DB} - k_{ox}\rho_{Char} \tag{2}$$

$$\frac{\partial \rho_{Ash}}{\partial t} = v_{Ash}k_{ox}\rho_{Char} \tag{3}$$

$$\frac{\partial \rho_{s}}{\partial t} = \frac{\partial \rho_{DB}}{\partial t} + \frac{\partial \rho_{Char}}{\partial t} + \frac{\partial \rho_{Ash}}{\partial t} = -v_{Vola}k_{devo}\rho_{DB} - (1 - v_{Ash})k_{ox}\rho_{Char} \tag{4}$$

Eq. (5) is employed to calculate the amount of released volatile, which will finally reflect to the heat releasing during volatile combustion process.

$$\frac{\partial \rho_{Vola}}{\partial t} = v_{Vola}k_{devo}\rho_{DB} \tag{5}$$

The moisture is considered as a separate liquid component in biomass, the drying process starts once the local temperature reaches the vaporisation temperature (T_b).

$$\frac{\partial m_M}{\partial t} = -k_{dry}m_M \tag{6}$$

The local moisture content is readily calculated by following equation:

$$\mathrm{MC} = \frac{\rho_{MC}}{\rho_s + \rho_{MC}} \tag{7}$$

The conservation of energy for the solid phase accounting accumulation, conduction, radiation, and heat released from both homogeneous and heterogeneous reactions is shown in Eq. (8).

$$\frac{\partial T_p}{\partial t}\left(\rho_M C_{P(M)} + \rho_{DB} C_{P(DB)} + \rho_{Char} C_{P(Char)} + \rho_{Ash} C_{P(Ash)}\right) = \frac{1}{r^2}\frac{\partial}{\partial r}\left(r^2 k' \frac{\partial T_p}{\partial r}\right) + \tilde{Q} \tag{8}$$

2.4. Devolatilization

The two-competing-rate model was employed to simulate the devolatilization process and predict the high temperature volatile matter yield [18]. In this model, the first reaction (A_1, E_1, and α_1) is used to calculate the devolatilization rate at lower temperatures, while the second reaction (A_2, E_2, and α_2) plays a dominant role at higher temperatures. The two kinetic rates are weighted to yield an expression of weight loss during the devolatilization process:

$$\frac{m_v(t)}{m_{p,0}} = \int_0^t (\alpha_1 k_1 + \alpha_2 k_2) \exp\left(-\int_0^t (k_1 + k_2)dt\right)dt \tag{9}$$

where $m_v(t)$ represents the mass of volatile is yield over the time, and $m_{p,0}$ is the initial particle mass at injection. The kinetic rates (k_1 and k_2) are expressed by the Arrhenius equations.

The particle diameter changes during devolatilization according to the swelling coefficient C_{sw}, and finally the particle diameter is calculated by the following equation:

$$\frac{d_p(t)}{d_{p,0}} = 1 + (C_{sw} - 1)\frac{(1 - f_{\omega,0})m_{p,0} - m_p}{f_{v,0}(1 - f_{\omega,0})m_{p,0}} \quad (10)$$

where $f_{\omega,0}$ is the initial moisture content of biomass; $f_{v,0}$ is the initial volatile content of studied biomass; and the term $\frac{(1-f_{\omega,0})m_{p,0}-m_p}{f_{v,0}(1-f_{\omega,0})m_{p,0}}$ is the ratio of the mass that has been devolatilized to the total volatile mass of the particle. If the swelling coefficient C_{sw} is equal to 2.0, the final particle diameter doubles after completion of devolatilization. While the swelling coefficient is equal to 0.5, the final particle diameter is half of its initial diameter. The swelling coefficients of coal are normally larger than 1, indicating its particle size increases during its devolatilization process; while swelling coefficients of biomass particles are usually less than 1, referring that the biomass particle size reduces during its devolatilization process. Swelling factor of the studied biomass was determined by morphological analysis, which is calculated as the ratio of the average diameter of char particles to the average diameter of the parent fuel. According to the morphological results, swelling factor of the studied biomass is 0.7. Due to the swelling properties of biomass particles are extremely difficult to be measured experimentally, uncertainty analysis of swelling factor, ranged from 0.5 to 1, is performed in this work.

2.5. Char oxidation

Char oxidation models are usually based on either apparent or intrinsic kinetics. In intrinsic kinetic approach, the char oxidation rate is related to the internal surface area of a char particle. The apparent kinetic have been frequently used under conditions limited by the combined effects of chemical kinetics and diffusion, to generally summarise the porous changes and also other thermal phenomenon within the reaction rate correlations. Due to the difficulty in determining the porous changes during biomass combustion process, the apparent kinetics is used in this work, and the char oxidation rates are predicted by the following equation [19]:

$$\frac{dm_p}{dt} = S_p k\left(P_{O_{2,\infty}} - \frac{dm_p}{dt}\frac{1}{S_p D}\right)^n \quad (11)$$

where m_p is the mass of the particle; S_p is the external surface area of the particle, which is calculated according to the particle size d_p; $P_{O_{2,\infty}}$ is the oxygen partial pressure; n is the apparent reaction order; k is the apparent kinetic rate; and D is the external diffusion rate coefficient calculated as follows [19]:

$$k = A_a \cdot \exp\left(-\frac{E_a}{RT}\right) \quad (12)$$

$$D = 2.57 \times 10^{-7}\frac{[(T_P + T_\infty)/2]^{0.75}}{d_p} \quad (13)$$

The evaluated diameter is modelled according to the following equation:

$$\frac{d_p}{d_{p,0}} = (1 - X)^{\alpha} \quad (14)$$

where A_a is the apparent pre-exponential factor, E_a is the apparent activation energy, d_p is the particle diameter (the subscript 0 indicates the initial value), and X is the degree of burnout. The limits of the burning mode are $0 \leqslant \alpha \leqslant \frac{1}{3}$, where $\alpha = 0$ refers to a constant particle size with a decreasing density (regime I), and $\alpha = \frac{1}{3}$ corresponds to a decreasing particle size with a constant density (regime III) throughout the conversion. However, in the regime II conditions, it is also important to note that the burning mode is a function of the particle size and combustion conditions. Due to the impacts of burning mode on the burnout prediction mainly at the late combustion stages, the burning mode is fixed to 0.25 in this simulation [20].

2.6. Numerical method, initial and boundary conditions

The mesh of studied particle includes a total of 40 layers along its radius, as presented in Fig. 2. Heating biomass particle is initially derived by the radiation and convective heat fluxes experienced on the particle surface, and then the temperature profile along the particle radius is calculated by energy equation (Eq. (8)). When the temperature at each note r_i is known, the reaction rates for each layer (dr_i) are calculated according to the average temperature ($\frac{r_i+r_{i+1}}{2}$), and then the total mass loss of biomass particle at time t are sum of mass losses of 40 individual layers. All the relevant physical properties and reaction kinetics used in this work are summarised in Table 2. Finally, the particle size is updated according to determined mass losses during for devolatilization and/or char oxidation process. Re-mesh of size-updated biomass particle will be carried out for next iteration at the time of ($t + \Delta t$), because the previous mesh would under/over cover the whole particle. Following this, the local temperature (T_i) does not represent the temperature at the same spatial point as previously represented. The partial differential equations (PDEs) were discretised by the finite volume method (FVM) to second-order accuracy.

At the beginning ($t = 0$), the particle temperature is at a room temperature (i.e. $T_{i,0} = 293$ K). The dry biomass density refers to the initial biomass density, the weight fractions of char increase when devolatilization starts. Fig. 2 also shows the boundary conditions at time $t > 0$. Neumann boundary conditions are used at both the particle centre and surface, with symmetrical effects considered at the particle centre ($r = 0$), as shown in Eq. (15); both the convection and radiative heat transfer are considered at the particle surface ($r = R$), as shown in Eq. (16).

$$\left.\frac{dT}{dr}\right|_{r=0} = 0 \quad (15)$$

$$\left.\frac{dT}{dr}\right|_{r=R} = h_c(T_\infty - T_p) + \omega\sigma\left(T_\infty^4 - T_p^4\right) \quad (16)$$

3. Results

3.1. Model validation

The devolatilization and char oxidation models have been validated by the experimental data characterised at high temperatures and high heating rates, as reported in previous work [15,16]. In both devolatilization and char oxidation studies, the biomass particles were collected and then analysed to determine the mass conversion according to the ash tracer method, which assumes ashes to be inert and thermally stable. Fig. 3a [16] shows that, although the model slightly overestimated the mass loss at the late stage of devolatilization at 1200 °C, while the model underestimated in a small degree the mass loss at the same stage of devolatilization at 900 °C, the predicted results have a good agreement with the experimental results at relatively high temperatures and the devolatilization model is able to predict accurately the total amount of released volatiles. Fig. 3b [15] examined the char oxidation model employed at varying temperature and oxygen concentrations. From Fig. 3b, at the temperature of 900 °C, the mass conversions of biomass char are under-predicted in the early stage of char oxidation, while the final mass conversions are slightly over-predicted when compared to the experimental data. When the temperature rises up to 1200 °C, a good agreement is achieved,

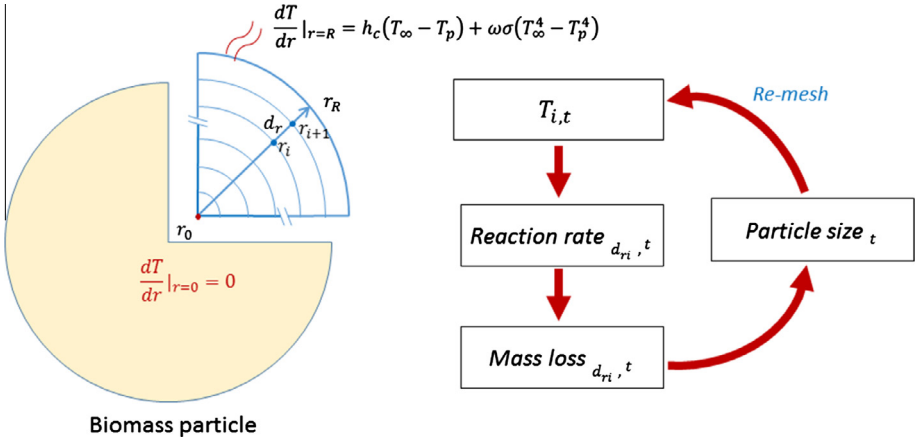

Fig. 2. The calculation scheme and boundary conditions.

Table 2
Physical properties and reaction kinetics for single particle combustion model.

	Correlation/value	Ref.
Dry biomass density	ρ_{DB} = 700 kg/m^3	
Dry biomass heat capacity	Cp_{DB} = 1112 + 4.85(T_p − 273.15) J/kg K	[21]
Char heat capacity	Cp_{Char} = 0.36 ∗ T_p + 1390 J/kg K	[21]
Moisture heat capacity	Cp_M = 4280 J/kg K	
Dry biomass thermal conductivity	$k'_{DB} = 0.13 + 0.0003(T_p - 273)$ W/m K	[22]
Char thermal conductivity	$k'_{Char} = 0.08 - 0.0001(T_P - 273)$ W/m K	[22]
Effective thermal conductivity	$k'_{eff} = \beta k'_{DB} + (1-\beta)k'_{Char}$ W/m K	[23]
Emissivity	ε = 0.95	[23]
Stefan–Boltzmann constant	$\sigma = 5.67 \times 10^{-8}$ $\frac{W}{m^2\ K^4}$	
Convection heat transfer coefficient	h = 8.4 W/m^2 K	[23]
Heat of vaporisation	$\Delta H^o_{evop} = 226$ kJ/kg	[24,25]
Heat required for devolatilization	H_{devo} = −418 kJ/kg	[24,25]
Heating released during char oxidation	H_{Char} = 32,800 kJ/kg	
Heating released during volatile oxidation	H_{vola} = LHV − H_{Char}(C − *Char*)/100	
Heat of reaction absorbed by solid residuals	$\widetilde{Q} = \sum_i \frac{\partial \rho_i}{\partial t} f_i H_i$ (i = drying, devolatilization, volatile combustion, char oxidation)	
Drying kinetics	$k_{dry} = 4.5 \times 10^3 \exp\left(-\frac{45{,}000}{RT_p}\right)$	[26]
Biomass devolatilization kinetics	$k_1 = 602 \exp\left(-\frac{42{,}500}{RT_p}\right)$ $k_2 = 8000 \exp\left(-\frac{130{,}000}{RT_p}\right)$ α_1 = 0.86 α_2 = 0.96	[16]
Coal devolatilization kinetics	$k_1 = 3.7 \times 10^5 \exp\left(-\frac{73{,}700}{RT_p}\right)$ $k_2 = 1.46 \times 10^{13} \exp\left(-\frac{251{,}000}{RT_p}\right)$ α_1 = 0.3 α_2 = 0.8	[27]
Biomass char oxidation kinetics	$k = 0.39 \exp\left(-\frac{47{,}500}{RT_p}\right)$, n = 0.29	[15]
Coal char oxidation kinetics	$k = 0.78 \exp\left(-\frac{946{,}000}{RT_p}\right)$, n = 1	[27]

although the predicted mass conversion is in a small degree lower than the experimental data, a good prediction for the final mass conversion is obtained. In consequence, the devolatilization and char oxidation models applied in this work are reasonable for further study on the prediction of devolatilization time and char burnout time.

3.2. Devolatilization time

Biomass normally has a higher volatile content than coal, and thus the devolatilization process assumes greater importance in the overall biomass combustion process. The devolatilization time of biomass with varying sizes is studied here at different oxygen concentrations and furnace temperatures, as shown in Fig. 4. The heating value of the volatiles is calculated based on the biomass heating value and proximate analysis data.

From Fig. 4, an enhanced oxygen concentration does not appear to accelerate the devolatilization process at the furnace temperatures of 700 °C and 900 °C. A higher furnace temperature promotes the devolatilization process, which is highly sensitive to the particle temperature, and the devolatilization rate is governed by the two competing rate models in this work. Results also show that a larger biomass particle requires a longer residence time to complete the devolatilization process, which is similar to the coal particle devolatilization according to the findings of Agarwal [3], where the devolatilization time is expressed as a function of the particle size and temperature:

$$\tau = k_v d_p^n \tag{17}$$

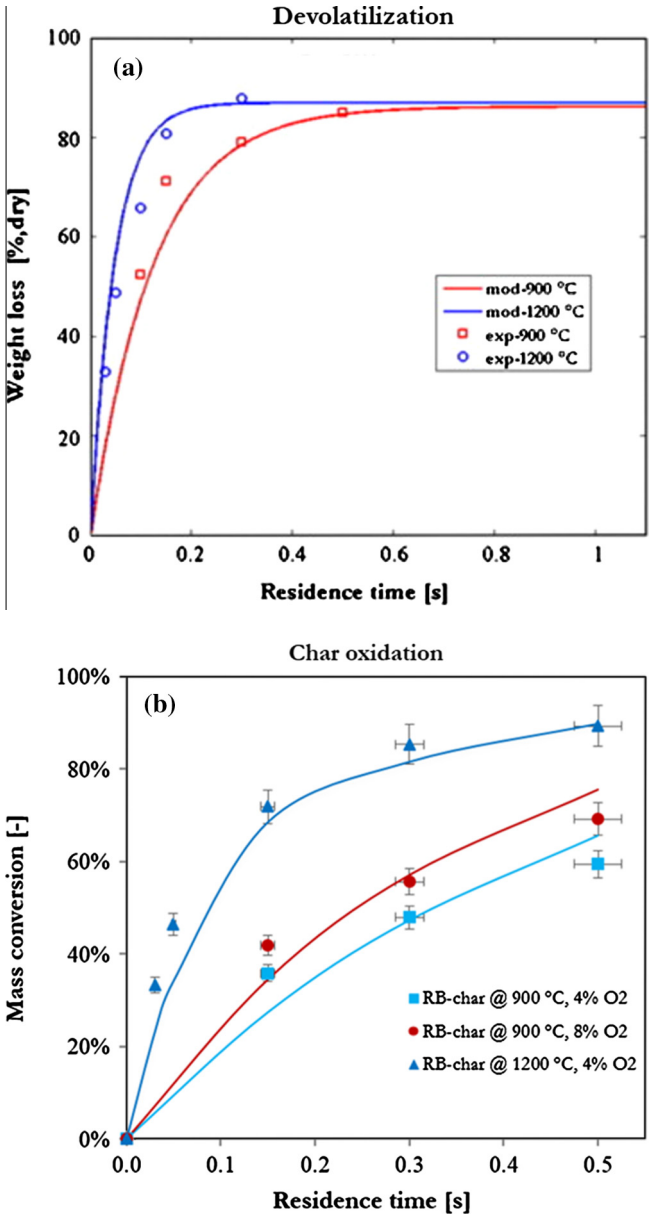

Fig. 3. Model validations for the studied biomass particles at high-temperature rapid processes (a. devolatilization [16]; b. char oxidation [15]).

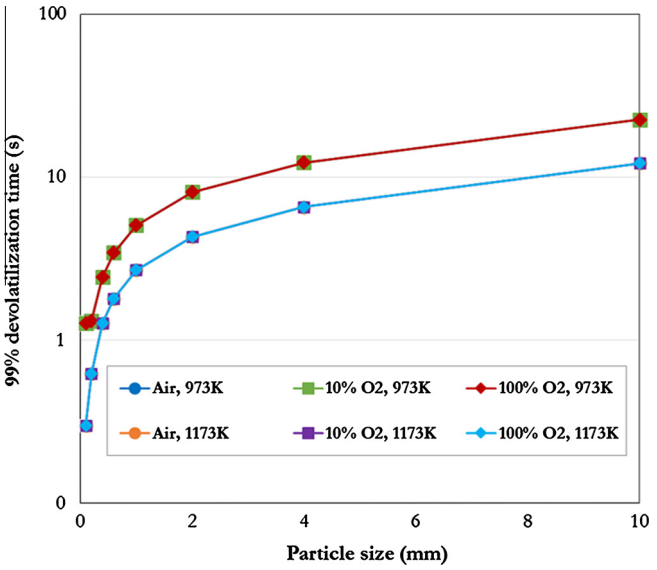

Fig. 4. Devolatilization time for biomass particles of different sizes at varying temperatures and oxygen concentrations.

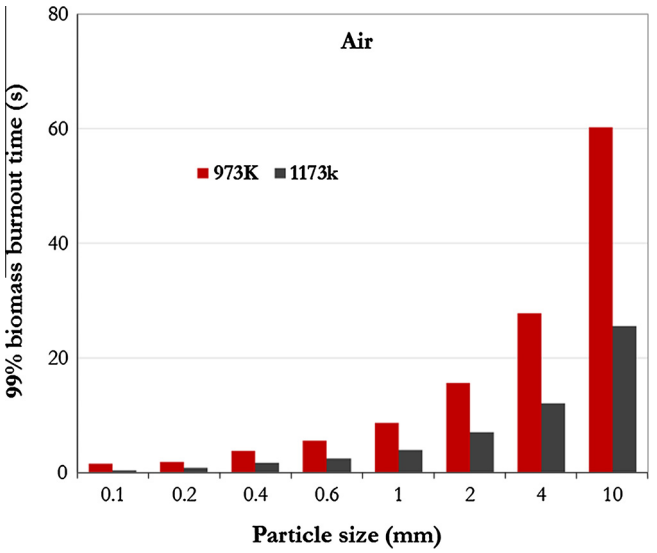

Fig. 5. Burnout time for biomass particles of different sizes at 700 and 900 °C.

k_v and n are constant and d_p is the coal particle diameter (mm). Agarwal reported that the effect of coal type on the devolatilization time τ is not strong when the particle size is larger than 0.5 mm. For the coal particle, it is suggested that k_v varies from 0.44 to 1.31, and n is 2. However, the incorporation of the swelling coefficient during the coal particle devolatilization process is neglected.

3.3. Combustion time

Total biomass combustion time is also studied in this work, represented by the biomass burnout time at 99% combustible content of biomass consumed. The total combustion time normally includes the heating up time, devolatilization time as well as char oxidation time. Fig. 5 generally shows that the burnout time of a biomass particle increases with an increase in particle size at 700 °C and 900 °C. An elevated temperature, apparently, shortens the total combustion time, and the combustion time at 900 °C is less than half that at 700 °C for all the studied biomass particles. For instance, it takes about 34.5 s to completely burn a 10 mm spherical biomass particle at the furnace temperature of 900 °C; when the furnace temperature drops to 700 °C, to complete the biomass combustion will take 60.3 s. The radiation is enhanced when increasing the furnace temperature, which significantly accelerates the devolatilization and the char burnout processes.

This work also addresses the impacts of oxygen concentration on the total biomass burnout time, as shown in Fig. 6. It is clear that an oxygen enrich atmosphere shortens the total combustion time for all the studied biomass, while a longer residence time is required to secure the completion of biomass char oxidation at a reduced oxygen atmosphere. For instance, when the furnace temperature is 900 °C, the total burnout time for a 10 mm woody biomass particle is about 33.31 s, 25.66 s, and 18.44 s at 10% oxygen, air, and pure oxygen combustion conditions, respectively. It is reasonable that, when the reactions are taken place at 900 °C or even higher temperatures, the Damköhler number (Da) becomes much greater than 1 and thus, the oxygen diffusion dominates the char

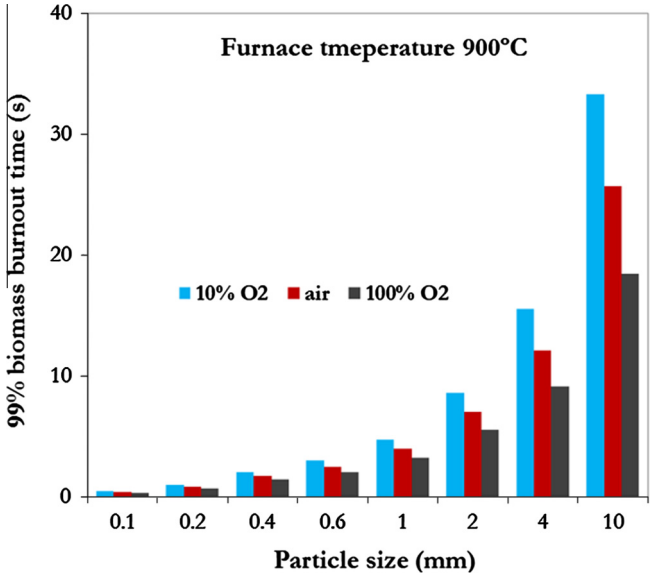

Fig. 6. Burnout time for biomass particles of different sizes at varying oxygen concentrations.

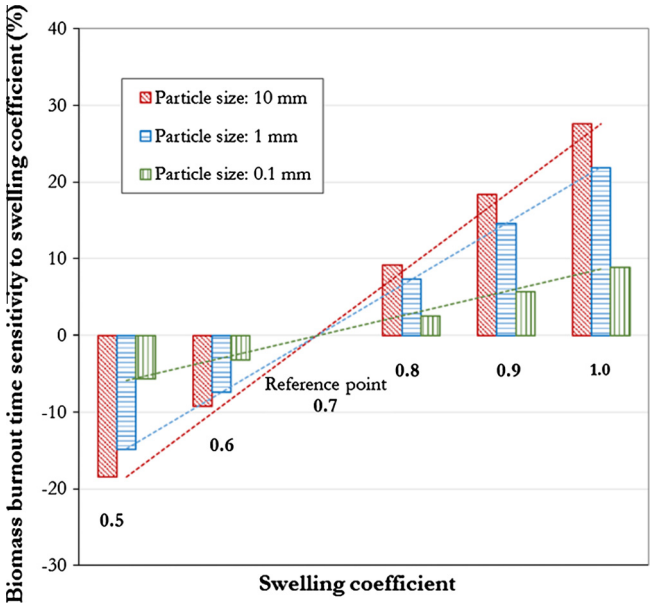

Fig. 7. Burnout time sensitivities to swelling coefficient.

oxidation rate resulting in a longer residence time to complete the char burnout process at 10% oxygen concentration. This also gives evidence that an existing coal-fired boiler with biomass co-firing could potentially achieve a better combustion performance and flame property, comparable to that of pure coal combustion, by modifying its oxygen concentrations inside the furnace.

4. Discussions

4.1. Characteristic time scales

A characteristic time scale analysis is commonly used to identify the dominant process occurring during the drying, devolatilization and char oxidation processes [28]. The time scales for the energy conservation inside the particle, the internal heat transfer, the chemical decomposition, and the external heat transfer at the surface are characterised. The relative importance of the internal heat transfer to the external heat transfer is defined by the ratio of their respective characteristic times, and a Biot number larger than 10 characterises the heat transfer limited by the internal conduction [28].

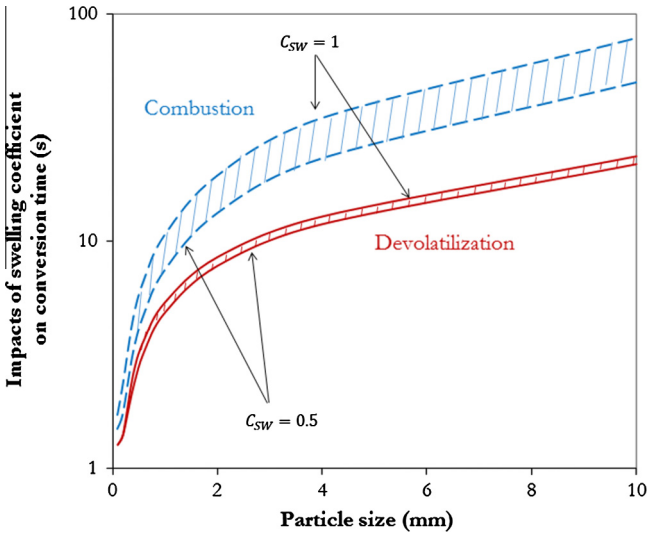

Fig. 8. The predictions of devolatilization and burnout time of biomass particles with swelling impacts.

In this work, a heating-up time of particle is well considered in the single particle model for all the studied particles ranging from 0.1 to 10 mm. The results show that, when compared to the time scale of the reaction completion, the heat transfer inside the particle reaches completes in a shorter time, even for the larger particles (10 mm). This could be explained by the reaction rate being highly temperature-dependent, while at high temperature it is likely controlled by diffusion and heat transfer. This case is therefore not only valid for fine particles but also for large particles.

4.2. Uncertainties over the swelling coefficient

Swelling behaviour normally occurs during biomass or coal devolatilization processes, and the swelling property depends on the fuel materials and devolatilization conditions (e.g. pressure and heating rates) [16,27,29,30]. However, biomass swelling properties are rarely characterised, which are extremely difficult to be obtained experimentally.

The volume shrinkage upon pyrolysis has been reported for a number of wood types [31,32], referring the swelling coefficient of wood particle is less than 1. Additionally, the morphological analysis has been performed on the studied biomass and its char; after completing devolatilization at 900 °C, its swelling coefficient is evaluated by comparing the average particle sizes of char and parent biomass. The determined swelling coefficient, 0.7, is employed to characterise the biomass particle changes during the devolatilization process, which is finally used as the reference point for the analysis of uncertainties. Fig. 7 presents the uncertainties of the swelling coefficient on the total biomass burnout time, and the swelling coefficient range is adapted from 0.5 to 1. Three different particle sizes (0.1, 1 and 10 mm) are studied, and the furnace temperature is fixed at 700 °C. The results show that a smaller swelling coefficient makes the biomass burnout time shorter, while a prolonged residence time is required to complete the combustion of biomass with a higher swelling index. This is explained by the fact that the surface reaction model is applied

to the large particles for the char oxidisation, and a larger particle requires more time to be burnout. However, the burnout time would be shorter than the predicted values because, in practice, the pyrolysis process normally promotes the formation of porosity, which ensures a high char reactivity [33,34].

In addition, Fig. 8 presents the predicted devolatilization time and biomass combustion time for different sizes biomass, considering the impacts of uncertainties of swelling coefficient. The results showed that total combustion time of larger biomass particle has much greater sensitivity to the swelling coefficient. For instance, taking the swelling coefficient of 0.7 as a reference value for the 10 mm biomass particle, the burnout time takes about 27.60% longer when the swelling coefficient increases to 1. Whereas, the burnout time is shorten by about 18.47% if the swelling coefficient drops to 0.5. Similarly to the 0.1 mm biomass particle, the burnout time changes +8.86% and −5.70% respectively when modifying the swelling coefficient to 1 and 0.5. This is caused by a low oxygen diffusion rate which depends on the particle diameter, as indicated in Eq. (11).

However, the devolatilization time is not significantly affected by the swelling coefficient for the large particles, as shown in Fig. 8. Compared to the case with a swelling coefficient of 0.5, a maximum time difference of 1.81 s was noticed for the largest particle devolatilization when the swelling coefficient increases to 1. However, the maximum biomass burnout time difference is also noticed for the largest particle case, which is about 28.24 s, and the impact of swelling is more significant on the total combustion time than that on the devolatilization. This could be explained by the devolatilization process being highly dependent on the temperature, while the swelling behaviour has less influence on the particle temperature profile. Compared to the devolatilization process, as discussed previously, the char oxidation could be affected by the temperature, particle size, and also by the oxygen diffusion rate. In addition, a range of devolatilization time and combustion time could be used to predict the biomass combustion behaviour either for biomass combustion or co-firing with coal in pulverized coal boilers.

4.3. Uncertainties of heat fraction of volatile combustion absorbed by solid

As mentioned before, due to the homogenous reaction rate is fast at high temperatures and the studies emphasises the devolatilization and char oxidation processes of solid, a single species of volatile is used to represent the all the produced gaseous species. These released volatiles react with oxygen in the vicinity of the char particles, increasing temperature and depleting the oxidizer (e.g., oxygen), hence the devolatilization and char oxidation processes might be accordingly accelerated. However, due to the difficulties in experimental determination of the heat fraction absorbed by solid, which may also change with varying the aerodynamic of gas flow, i.e. gas flow velocity, an uncertainty analysis of the heat fractions of volatile combustion absorbed by solid has been carried out to address its impacts.

Two extreme cases are studied: (1) the heat released from volatile combustion is not transferred to solid considering a fast air injection velocity, in this case, volatile combustion occurs far away from the vicinity of solid surface; (2) the heat released from volatile combustion is 100% absorbed by solid considering a stationary air inside a isothermal furnace, in this case, volatile combustion happens completely at the surface of solid. However, both cases mentioned above are not existed in practice, the studies carried out on those two cases are aiming for investigating the impacts of homogeneous reactions on the devolatilization and total burnout time.

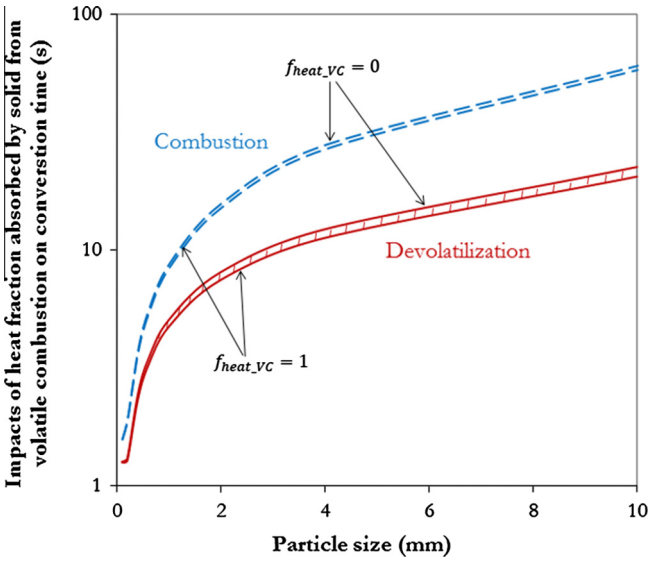

Fig. 9. The predictions of devolatilization and burnout time of biomass particles with gas-reaction heat fraction absorbed by solid impacts.

Fig. 9 presents the predicted devolatilization time and biomass combustion time for different sizes of biomass, as a base case, without considering the impacts of heat absorption of solid from volatile combustion. The minus error bars in Fig. 9 show the devolatilization and total combustion time changes when the heat released from volatile combustion is fully absorbed by solid. It is noticed that both the devolatilization and total combustion processes of biomass particle are accelerated, but the acceleration rate is limited, especially for the entire biomass combustion process. With the increasing of biomass particle size, the impacts of heat absorption by solid from the volatile combustion become more important, and thus the conversion time differences between the studied two cases are getting longer. For fine particles, e.g. 0.1 mm, both the devolatilization and total combustion time are shorten by −0.01 s, which means that the char oxidation is not affected by heats released from volatile combustions. While for the largest biomass particle, 10 mm, the devolatilization and total combustion time are shorten by 2.01 s and 2.15 s, respectively, indicating that the reaction rate acceleration is mainly acted in the devolatilization process, while the rate acceleration in char oxidation is also able to be noticed but at a neglect level.

4.4. Biomass combustion option

Combustion properties of biomass are significantly different from those of coals due to high volatile contents and low energy densities. Li et al. [35] compared the biomass flame with that of coal and concluded that the enhanced drag force on the biomass particles results in a longer lift-off distance and the flame is far from the burner injection. Delayed combustion may cause the major combustion zone of the biomass to move towards the furnace exit in a pulverized co-firing boiler, probably causing an unexpected overheating of platen super-heaters [27]. To enlarge the biomass co-firing ratio in a coal-fired boiler, a biomass flame is expected to be similar to a coal flame.

In this work, a ratio of the devolatilization time to that of the combustion is defined and employed to understand the biomass combustion performance at various operating conditions, and results are compared with those of coal, as shown in Fig. 10. The biomass combusted with air at 900 °C is used as the reference case. Two cases are kept at the same temperature of 900 °C but with dif-

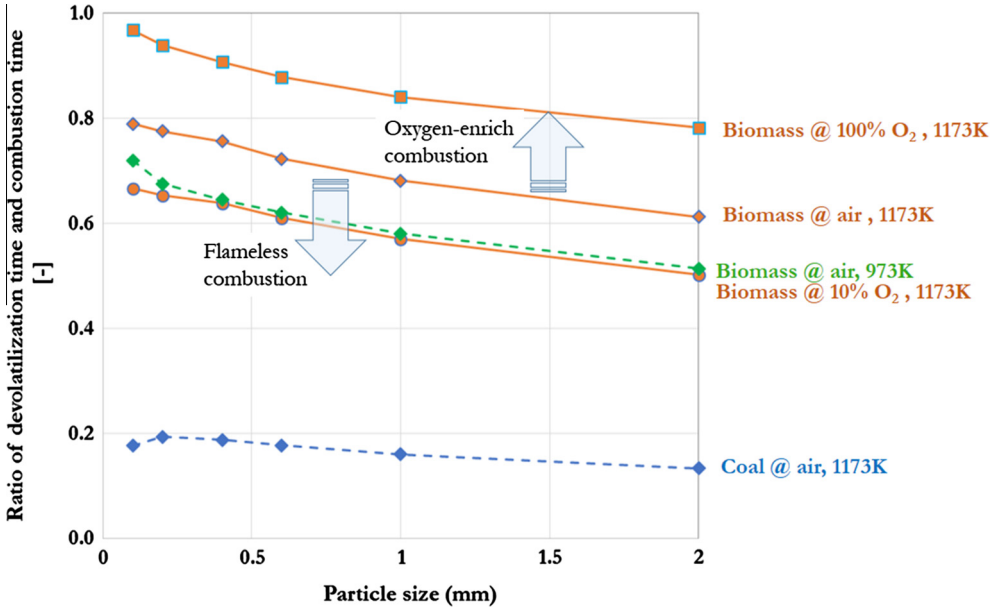

Fig. 10. Comparison of ratio of the devolatilization time to total combustion time at various conditions.

ferent oxygen concentrations: pure oxygen and 10% oxygen concentration. Another case maintains the air atmosphere but at reduced temperature of 700 °C. The case of coal combustion with air at 900 °C is used for comparison. Fig. 10 shows the ratio of the devolatilization time to the burnout time reduces when the particle size is increased because the larger particle requires a longer residence time to complete the char oxidation process, while the impacts of particle size on devolatilization time do not change much, which is governed by temperature and thus depends the heating up rate of biomass particle. In addition, when combustion occurs with air at the same temperature of 900 °C, the ratio for the biomass particles with the studied particle size becomes much higher than that of the coals. A major factor contributing to this is the small volatile content of coals compared to the biomass, as presented in Table 1. Another reason might be the different fuel properties indicated by the different kinetic parameters of biomass and coal.

Furthermore, Fig. 10 indicates that an enriched oxygen concentration shifts the ratio of the devolatilization time to the total combustion time even far away from the coal curve, resulting in biomass flames being far different from coal flames. However, reducing both the furnace temperature and the oxygen concentration can move the ratio towards that of coal, thus yielding a biomass flame more similar to a coal flame and providing a potential solution for large percentage biomass co-firing in coal-fired boilers. Interestingly, a reduced peak flame temperature and oxygen concentration can be realised by a flameless combustion/high temperature air combustion (HiTAC) approach, which has been proposed initially to reduce NOx emissions [36,37]. In consequence, from the combustion point of view, the flameless combustion scheme could also be a solution for the biomass co-firing with a good combustion performance and be able to reach a large biomass substitution ratio in existing pulverized coal-fired boilers.

5. Conclusions

A comprehensive single particle model has been employed and upgraded for high-temperature rapid biomass combustion studies. The biomass devolatilization reaction was simulated by a two-competing-rate model and the biomass char burnout rate was controlled by both the kinetics and diffusion, taking the particle size changes during the devolatilization and char oxidation processes. The results showed that the elevated temperature significantly enhanced the biomass mass loss at the devolatilization stage; while a longer residence time was required to completely burnout char. In addition, the oxygen-rich condition does not affect the devolatilization time of the selected woody biomass, but it affects significantly the char oxidation process. When the biomass combusted at a reduced oxygen concentration or a lower furnace temperature, the ratio of the devolatilization time to the burnout is decreased and this moves towards the ratios of coal. And accordingly, flameless combustion scheme could be a solution for biomass co-firing with coal in existing coal-fired boilers to archive a better combustion performance.

Acknowledgements

Financial support for this research from The Carnegie Trust and EPSRC (EP/K503903/1) through an Impact Acceleration Award is gratefully acknowledged.

References

[1] Saxena SC, Jotshi CK. Fluidized-bed incineration of waste materials. Prog Energy Combust Sci 1994;20:281–324.
[2] Johnson GR, Murdoch P, Williams A. A study of the mechanism of the rapid pyrolysis of single particles of coal. Fuel 1988;67(6):834–42.
[3] Agarwal PK. A single particle model for the evolution and combustion of coal volatiles. Fuel 1986;65(6):803–10.
[4] Ballal G, Li C-H, Glowinski R, Amundson NR. Single particle char combustion and gasification. Comput Methods Appl Mech Eng 1989;75(10):467–79.
[5] Morell JI, Amundson NR, Park SK. Dynamics of a single particle during char gasification. Chem Eng Sci 1990;45:387–401.
[6] Goshayeshi B, Sutherland JC. A comparison of various models in predicting ignition delay in single-particle coal combustion. Combust Flame 2014;161(7):1900–10.
[7] Wurzenberger JC, Wallner S, Raupenstrauch H, Khinast JG. Thermal conversion of biomass: comprehensive reactor and particle modeling. AIChE J 2002;48:2398–411.
[8] Porteiro J, Granada E, Collazo J, Patiño D, Morán JC. A model for the combustion of large particles of densified wood. Energy Fuels 2007;21:3151–9 (2007/11/01).
[9] Porteiro J, Míguez JL, Granada E, Moran JC. Mathematical modelling of the combustion of a single wood particle. Fuel Process Technol 2006;87(1):169–75.
[10] Haseli Y, van Oijen JA, de Goey LPH. A detailed one-dimensional model of combustion of a woody biomass particle. Bioresour Technol 2011;102(10):9772–82.

[11] Lu H, Ip E, Scott J, Foster P, Vickers M, Baxter LL. Effects of particle shape and size on devolatilization of biomass particle. Fuel 2010;89(5):1156–68.
[12] Lu H, Robert W, Peirce G, Ripa B, Baxter LL. Comprehensive study of biomass particle combustion. Energy Fuels 2008;22:2826–39 [2008/07/01].
[13] Saastamoinen J, Aho M, Moilanen A, Sørensen LH, Clausen S, Berg M. Burnout of pulverized biomass particles in large scale boiler – single particle model approach. Biomass Bioenergy 2010;34(5):728–36.
[14] Yang YB, Sharifi VN, Swithenbank J, Ma L, Darvell LI, Jones JM, et al. Combustion of a single particle of biomass. Energy Fuels 2007;22:306–16 [2008/01/01].
[15] Li J, Bonvicini G, Biagini E, Yang W, Tognotti L. Characterization of high-temperature rapid char oxidation of raw and torrefied biomass fuels. Fuel 2015;143:492–8 [3/1/].
[16] Li J, Bonvicini G, Tognotti L, Yang W, Blasiak W. High-temperature rapid devolatilization of biomasses with varying degrees of torrefaction. Fuel 2014;122:261–9 (4/15/).
[17] Li J, Jankowski R, Kotecki M, Yang W, Szewczyk D, Brzdekiewicz A, et al. CFD approach for unburned carbon reduction in pulverized coal boilers. Energy Fuels 2011;26:926–37 [2012/02/16].
[18] Kobayashi H, Howard JB, Sarofim AF. Coal devolatilization at high temperatures. In: Symposium (International) on combustion, vol. 16; 1977. p. 411–25.
[19] Morgan ME, Roberts PA. Coal combustion characterisation studies at the international flame research foundation. Fuel Process Technol 1987;15:173–87.
[20] Karlström O, Brink A, Hupa M, Tognotti L. Multivariable optimization of reaction order and kinetic parameters for high temperature oxidation of 10 bituminous coal chars. Combust Flame 2011;158(10):2056–63.
[21] Grieco E, Baldi G. Analysis and modelling of wood pyrolysis. Chem Eng Sci 2011;66:650–60.
[22] Koufopanos CA, Papayannakos N, Maschio G, Lucchesi A. Modelling of the pyrolysis of biomass particles. Studies on kinetics, thermal and heat transfer effects. Can J Chem Eng 1991;69:907–15.
[23] Babu BV, Chaurasia AS. Heat transfer and kinetics in the pyrolysis of shrinking biomass particle. Chem Eng Sci 2004;59(5):1999–2012.
[24] Blasi CD. Dynamic behaviour of stratified downdraft gasifiers. Chem Eng Sci 2000;55:2931–44. 8/1/.
[25] Di Blasi C. Modeling wood gasification in a countercurrent fixed-bed reactor. AIChE J 2004;50:2306–19.
[26] Bates RB, Ghoniem AF. Modeling kinetics-transport interactions during biomass torrefaction: the effects of temperature particle size and moisture content. Fuel 2014;137:216–29. 12/1/.
[27] Li J, Brzdekiewicz A, Yang W, Blasiak W. Co-firing based on biomass torrefaction in a pulverized coal boiler with aim of 100% fuel switching. Appl Energy 2012;99(11):344–54.
[28] Chan W-CR, Kelbon M, Krieger BB. Modelling and experimental verification of physical and chemical processes during pyrolysis of a large biomass particle. Fuel 1985;64(11):1505–13.
[29] Lee CW, Scaroni AW, Jenkins RG. Effect of pressure on the devolatilization and swelling behaviour of a softening coal during rapid heating. Fuel 1991;70 (8):957–65.
[30] Fletcher TH. Swelling properties of coal chars during rapid pyrolysis and combustion. Fuel 1993;72(11):1485–95.
[31] Byrne CE, Nagle DC. Carbonized wood monoliths—characterization. Carbon 1997;35:267–73.
[32] Davidsson KO, Pettersson JBC. Birch wood particle shrinkage during rapid pyrolysis. Fuel 2002;81(2):263–70.
[33] González JF, Román S, Encinar JM, Martínez G. Pyrolysis of various biomass residues and char utilization for the production of activated carbons. J Anal Appl Pyrol 2009;85(5):134–41.
[34] Stratford JP, Hutchings TR, de Leij FAAM. Intrinsic activation: the relationship between biomass inorganic content and porosity formation during pyrolysis. Bioresour Technol 2014;159(5):104–11.
[35] Li J, Biagini E, Yang W, Tognotti L, Blasiak W. Flame characteristics of pulverized torrefied-biomass combusted with high-temperature air. Combust Flame 2013;160(11):2585–94.
[36] Li J, Yang W, Blasiak W, Ponzio A. Volumetric combustion of biomass for CO_2 and NOx reduction in coal-fired boilers. Fuel 2012;102(12):624–33.
[37] Wünning JA, Wünning JG. Flameless oxidation to reduce thermal no-formation. Prog Energy Combust Sci 1997;23:81–94.